Supplemental Information

Activation of P-TEFb by androgen receptor-regulated enhancer RNAs in castration-resistant prostate cancer

Yu Zhao, Liguo Wang, Shancheng Ren, Lan Wang, Patrick R. Blackburn, Melissa S. McNulty, Xu Gao, Meng Qiao, Robert L. Vessella, Manish Kohli, Jun Zhang, R. Jeffrey Karnes, Donald J. Tindall, Youngsoo Kim, Robert MacLeod, Stephen C. Ekker, Tiebang Kang, Yinghao Sun and Haojie Huang

Supplemental Fig.1

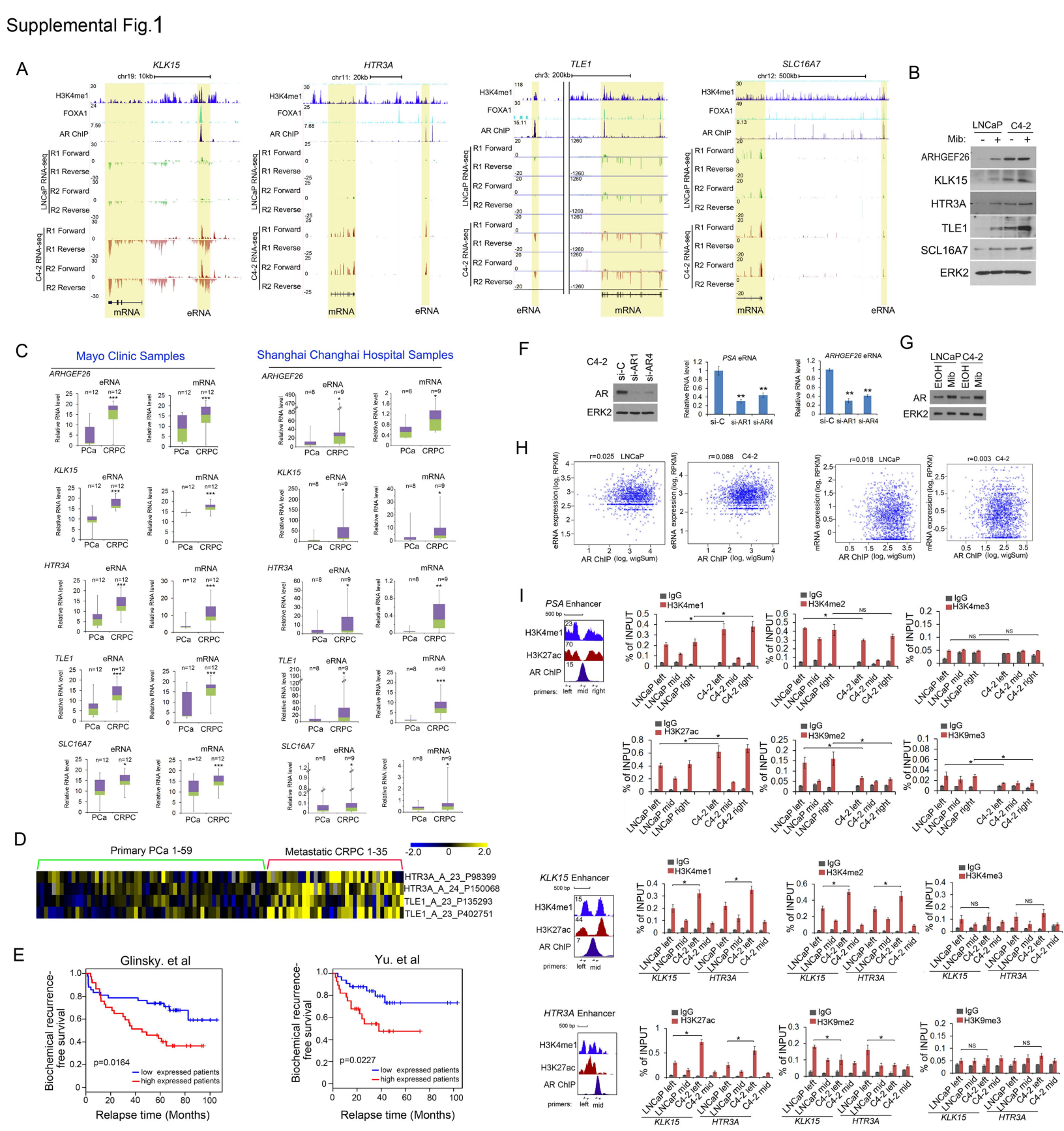

Figure S1. AR-eRNAs are upregulated at the gene loci *KLK15, HTR3A, TLE1* and *SLC16A7* in CRPC cells in culture. **Related to Figure 1 and 2**

(A) Screen shots from the UCSC genome browser showing signal profiles of eRNA expression (strand-specific RNA-seq) in LNCaP and C4-2 and AR ChIP-seq in LNCaP as well as H3K4me1 and FOXA1 ChIP-seq data from LNCaP cells reported previously (Wang et al., 2011). The eRNA and mRNA regions are highlighted in yellow.

(B) Protein expression of five new AR target genes (*ARHGEF26*, *KLK15*, *HTR3A*, *TLE1* and *SLC16A7*) was measured by western blot in LNCaP and C4-2 cells treated with or without 10 nM of synthetic androgen mibolerone (Mib).

(C) eRNA and mRNA expression of five new AR target genes in human CRPC tissues. eRNA and mRNA expression of *ARHGEF26, KLK15, HTR3A, TLE1 and* SLC16A7 was measured by RT-qPCR in human primary hormone-naïve prostate cancer (PCa) and CRPC tissues. Tissues from Mayo Clinic were paraffin embedded and those from Shanghai Changhai Hospital were fresh frozen tissues. Outliers were omitted from box plots. * $P < 0.05$; ** $P < 0.01$; *** $P < 0.001$**.**

(D) Heat map of expression of *HTR3A* and *TLE1* mRNAs in a cohort of human hormone-naïve primary prostate cancer (PCa) and metastatic CRPC tissues reported by Grasso et al (Grasso et al., 2012).

(E) Kaplan-Meier plots showing the power of the AR new target genes in predicting biochemical recurrence. Datasets are reported by Glinky et al. (Glinsky et al., 2005) (ARHGEF26 gene probe(s) were not found in the dataset) (C) and by Yu et al., (Yu et al., 2004) (ARHGEF26 and KLK5 gene probe(s) were not found in the dataset) (D).

(F) AR knockdown decreased expression of AR-eRNAs (*PSA* and *ARHGEF26* eRNAs) in C4-2 cells. AR protein and *PSA* and *ARHGEF26* eRNA expression were examined by western blot and RT-qPCR, respectively. Means and standard deviations (error bar) were determined from three replicates. ** $P < 0.05$.

(G) AR protein expression was examined by western blot in LNCaP and C4-2 cells treated with or without 10 nM of Mibolerone (Mib).

(H) Genome-wide analysis of correlation between AR binding at 1,865 enhancers and eRNA (or mRNA) expression at corresponding AR-bound enhancers in LNCaP and C4-2 cells. Each dot represents a putative enhancer with detectable eRNA expression and AR binding. The *r* value represents the Spearman correlation coefficient.

(I) Left, schematic diagram showing the locations (at the *PSA*, *KLK15* and *HTR3A* enhancers) of the PCR primers that were designed based signal peaks of AR, H3K4me1 and H3K27ac ChIP-seq data. Right, ChIP-qPCR analysis of H3K4me1, H3K4me2, H3K4me3, H3K27ac, H3K9me2 and H3K9me3 at the *PSA, KLK15* and *HTR3A* enhancers in LNCaP and C4-2 cells. All data shown are mean values ± SD (error bar) from three replicates. * $P < 0.05$. NS, no significant difference.

Supplemental Fig. 2

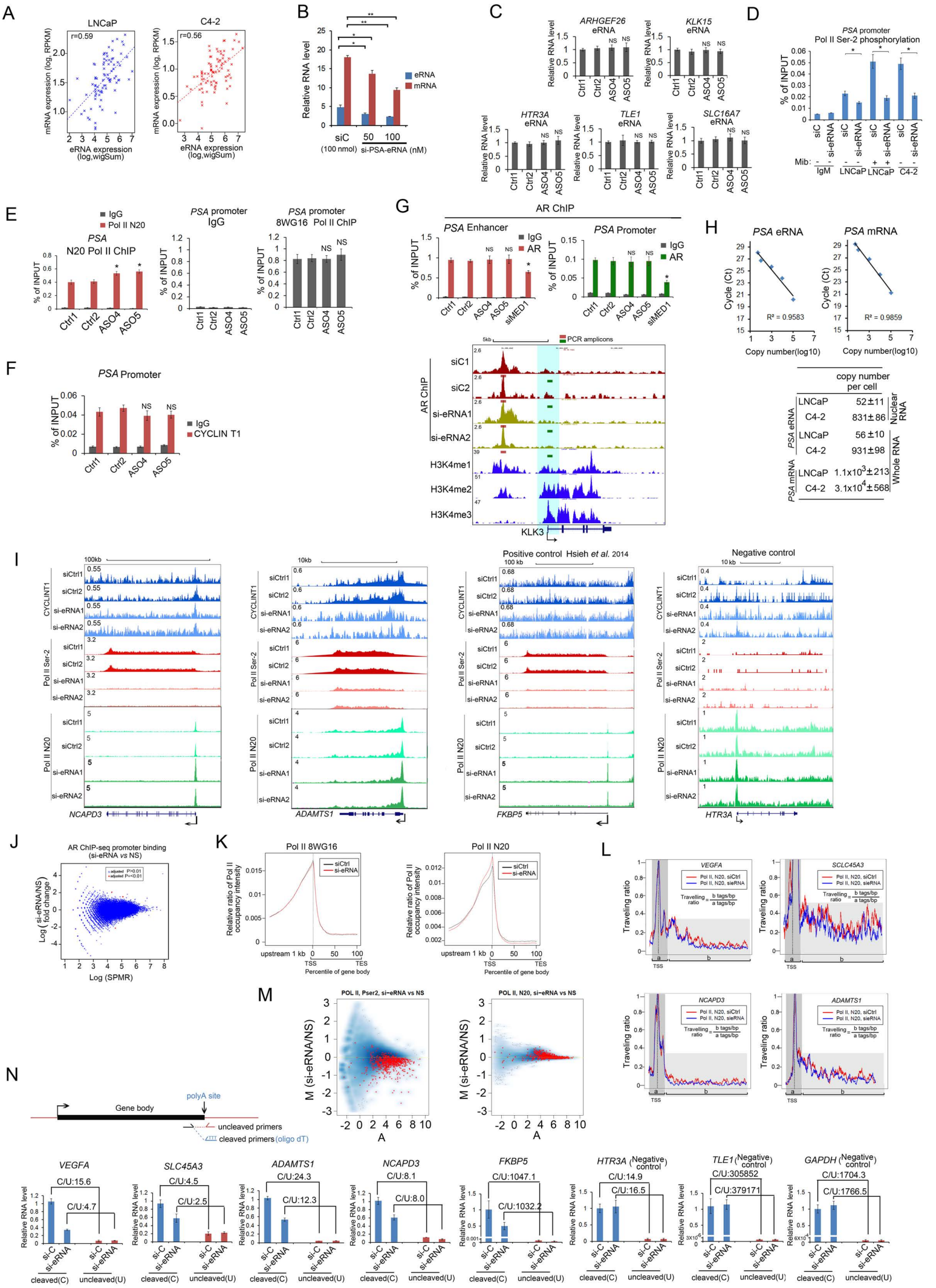

Figure S2. Effects of *PSA* eRNA on Pol II Ser-2 phosphorylation, total Pol II and AR binding at the *PSA* locus. Related to Figure 3

(A) Genome-wide correlation between expression of AR-eRNAs and corresponding mRNAs of 1,865 AR target genes in LNCaP and C4-2 cells. Each dot represents a set of genes that have similar mRNA induction and a corresponding set of enhancers nearby those genes using the method as described previously (Grasso et al., 2012). The *r* value represents the Spearman correlation coefficient.

(B) Measurement of *PSA* eRNA and mRNA expression by RT-qPCR in C4-2 cells transfected with control (siC) or *PSA* eRNA-specific siRNAs. All data shown are mean values ± SD (error bar) from three replicates. * $P < 0.05$; ** $P < 0.01$.

(C) Effect of *PSA* eRNA knockdown mediated by eRNA-specific ASOs on other AR-eRNA expression. Expression of eRNAs of indicated genes was measured by RT-qPCR. All data shown are mean values ± SD (error bar) from three replicates. NS, no significant difference.

(D - F) ChIP-qPCR analysis of Pol II Ser-2 phosphorylation (D), total Pol II (N20) (E, left), unphosphorylated Pol II (8WG16) (E, middle and right), and CYCLIN T1 binding (F) at the *PSA* gene promoter or enhancer in C4-2 cells transfected with control or *PSA* eRNA-specific siRNA or C4-2 cells transfected with control or *PSA* eRNA-specific ASOs. Immunoprecipitated DNA was detected by real-time PCR. All data shown are mean values ± SD (error bar) from three replicates. * $P < 0.01$. NS, no significant difference.

(G) Top, AR binding at the *PSA* gene promoter or enhancer in C4-2 cells transfected with control or MED1-specific siRNA or C4-2 cells transfected with control or *PSA* eRNA-specific ASOs. Immunoprecipitated DNA was detected by real-time PCR. All data shown are mean values ± SD (error bar) from three replicates. * $P < 0.01$. Bottom, screen shots from the UCSC genome browser showing signal profiles of AR ChIP-seq in the *PSA* locus in C4-2 cells transfected with control (siC) and PSA eRNA-specific siRNA (si-eRNA) and histone ChIP-seq in LNCaP cells, which was reported previously (Wang et al., 2011). The promoter regions of *PSA* are highlighted in light blue. PCR product sites in the enhancer and promoter of *PSA* are highlighted in red and green, respectively.

(H) The titration curve was used to measure the copy numbers of *PSA* eRNA in the whole cell or nuclear extracts of LNCaP and C4-2 cells using RT-qPCR.

(I) Screen shots from the UCSC genome browser showing signal profiles of Pol II Ser-2 phosphorylation, total Pol II signals and CYCLIN T1 binding (ChIP-seq) from two biological replicates. *FKBP5* reported recently by Hsieh et al., (Hsieh et al., 2014) and *HTR3A* were used as a positive and negative control, respectively.

(J) Differential AR binding at promoters genome wide. The promoter of a particular gene is defined as the 2-kb region centered on its transcription start site (TSS). X-axis denotes the normalized read count (i.e. Reads Per Million mapped reads or RPM). Y-aixs is the fold change of RPM between NS and si-eRNA experiments. Red dots represent promoters showing significantly changed AR binding (adjusted $P <= 0.01$), and blue dots represent promoters showing no significantly changed AR binding (adjusted $P > 0.01$). Differential binding analysis was performed using EdgeR.

(K) ChIP-seq tag intensity profiles of unphosphorylated Pol II (8WG16) (left) and total Pol II (N20) (right) at 674 target loci in C4-2 cells with or without *PSA* eRNA knockdown. X-axis indicates the gene body and upstream 1 Kb region. Y-axis indicates relative ratio of Pol II occupancy intensity calculated as reads intensity at each position divided by the total read intensity of the gene. All genes annotated by RefSeq were scaled into the same length by picking 100 points with equal intervals from TSS to transcription end site (TES).

(L) The total Pol II traveling ratio was calculated as the ratio of total Pol II density of the gene body (b = +100 bp to 10,000 bp) to the average Pol II density within the proximal promoter (a = -100 bp to + 100 bp) in C4-2 cells. The dashed vertical line in each gene indicates the TSS.

(M) MA plots showing the difference of ChIP-seq reads intensity between control (NS) and eRNA knocking down (si-eRNA) conditions for Pol II Ser-2p (left) and N20 (right). Gene body is defined as +500 from TSS to TES. ChIP-seq signal of each gene was measured by "reads per million" or RPM (i.e. number of reads mapped to a particular gene is normalized by total reads). Smoothed scatter plots were used to represent the background distribution of all genes with the 674 changed loci (red cross) superimposed on top. Both X and Y-aixs are log2 scaled after calculating A (averaged RPM) and M (ratio of RPM between si-eRNA and control).

(N) Effect of *PSA* eRNA on 3' cleavage efficiency of *trans* target mRNAs examined in C4-2 CRPC cells. All data shown are mean values ± SD (error bar) from three replicates.

Supplemental Fig. 3

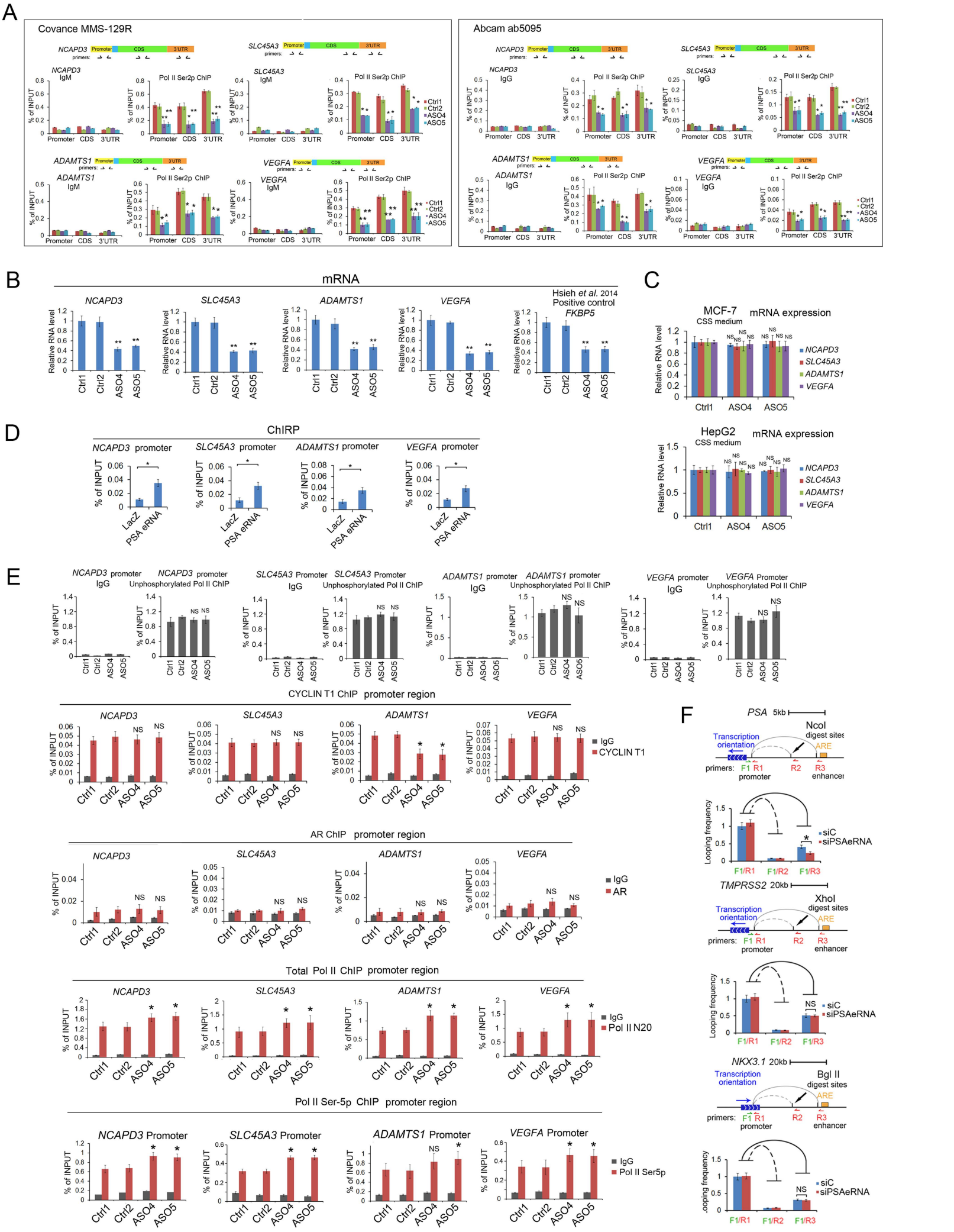

Figure S3. Effects of *PSA* eRNA on Pol II Ser-2 phosphorylation, total Pol II, AR and CYCLIN T1 binding at the *PSA* locus. Related to Figure 3

(A) ChIP-qPCR analysis of Pol II Ser2 phosphorylation at target gene loci in C4-2 cells. Immunoprecipitated DNA was detected by real-time PCR. All data shown are mean values ± SD (error bar) from three replicates. * $P < 0.05$; ** $P < 0.01$.

(B) Effect of *PSA* eRNA on mRNA expression of *trans* targets examined in C4-2 CRPC cells. All data shown are mean values ± SD (error bar) from three replicates. ** $P < 0.01$.

(C) Effect of *PSA* eRNA on mRNA expression of *trans* targets examined in MCF-7 breast cancer and HepG2 liver cancer cell lines. All data shown are mean values ± SD (error bar) from three replicates. NS, no significant difference.

(D) ChIRP assay using biotin-labeled LacZ or *PSA* eRNA-specific DNA probes and streptavidin beads. Pulldown DNA was analyzed by real-time PCR. All data shown are mean values ± SD (error bar) from three replicates. * $P < 0.05$.

(E) ChIP-qPCR analysis of total Pol II (N20), unphosphorylated Pol II (8WG16), CYCLIN T1 and AR at the indicated *trans* target gene promoters of *PSA* eRNA in C4-2 cells. Immunoprecipitated DNA was detected by real-time PCR. All data shown are mean values ± SD (error bar) from three replicates. * $P < 0.05$. NS, no significant difference.

(F) Evaluation of the enhancer-promoter interaction at *PSA*, *TMPRSS2* and *NKX3.1* loci by chromosome conformation capture (3C) assays. Solid line and dotted line show different digest sites. * $P < 0.05$. NS, no significant difference.

Supplemental Fig. 4

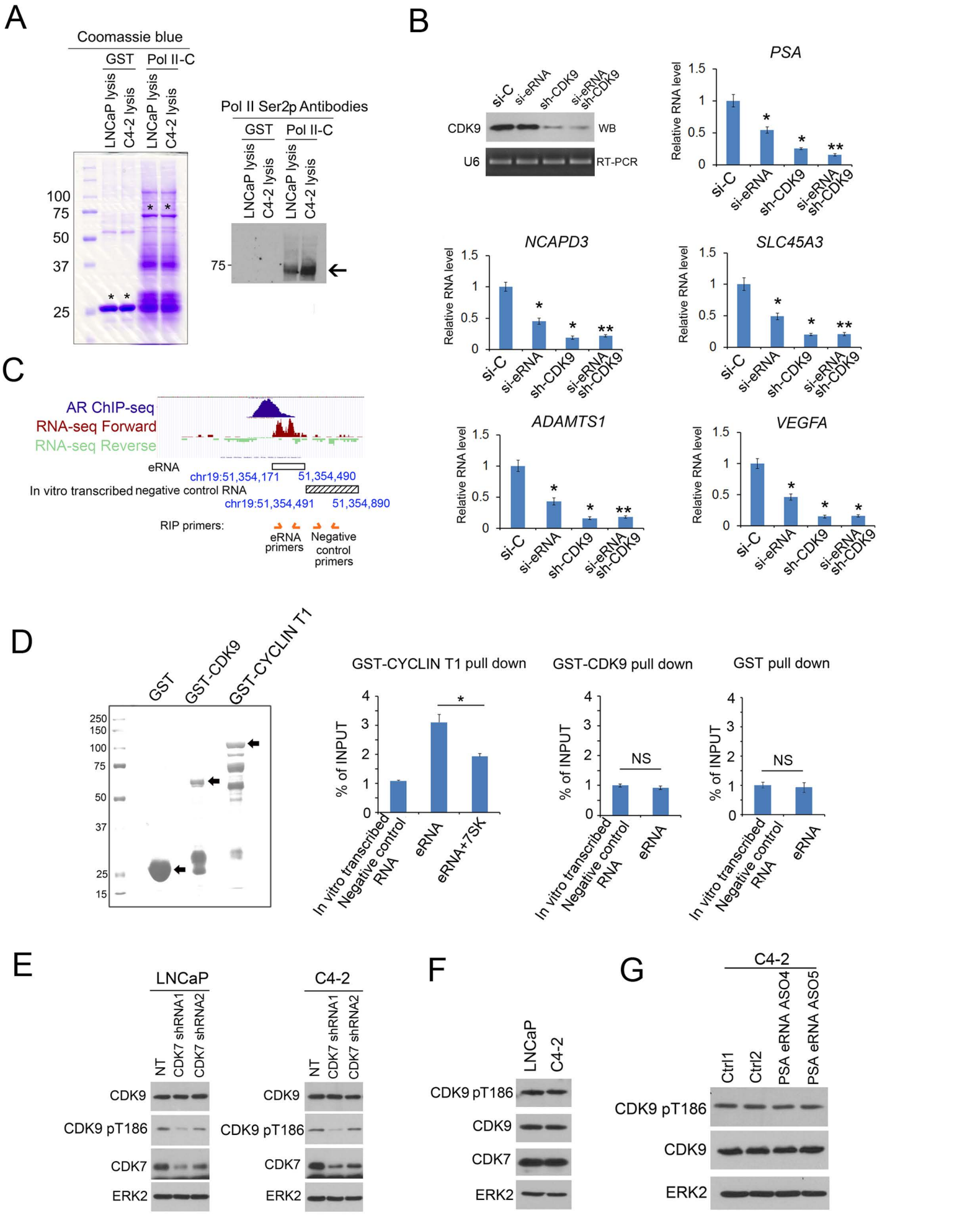

Figure S4. Analysis of Pol II-Ser2 phosphorylation, P-TEFb activity, CDK9 T-loop phosphorylation and *PSA* eRNA binding with CYCLIN T1. Related to Figure 4

(A) Left, Coomassie blue staining of GST and GST-Pol II-C terminal domain recombinant proteins used for kinase assay. Asterisks indicate the GST and GST-Pol II-C recombinant protein bands. Right, determination of CTD kinase (CDK9) activity. 1 μg GST or GST-Pol II-C proteins were incubated with CDK9 immunoprecipitated from LNCaP and C4-2 cells for kinase assay. After extensive washing, GST-beads were collected and subject to SDS/PAGE and western blot with Pol II Ser-2p antibodies.

(B) mRNA expression of *PSA* and the *trans* genes of *PSA* eRNA were measured by RT-qPCR in C4-2 cells with or without knockdown of *PSA* eRNA, CDK9 or both. U6 was used as an internal control. Data shown as means±SD (n=3). * $P < 0.05$ and ** $P < 0.01$ comparing to the control siRNA (siC) group.

(C) A diagram indicating the locations of *PSA* eRNA peaks detected by RNA-seq and a downstream non-peak region relative to the AR ChIP peak in the *PSA* enhancer.

(D) Left, Coomassie blue staining of GST, GST-CDK9 and GST-CYCLIN T1 recombinant proteins purified from bacteria. Right, *in vitro* GST pulldown assays were performed by incubating RNAs *in vitro* transcribed from the *PSA* eRNA peak region or negative control region. Pulldown RNAs were analyzed by RT-qPCR. All data shown are mean values ± SD (error bar) from three replicates. * $P < 0.05$. NS, no significant difference.

(E-G) Expression of CDK9, CDK7, CDK9 T186p and ERK2 proteins were measured by western blot in LNCaP and C4-2 cells infected with control or CDK7-specific shRNAs or in C4-2 cells transfected with control or *PSA* eRNA-specific ASOs.

Supplemental Fig. 5

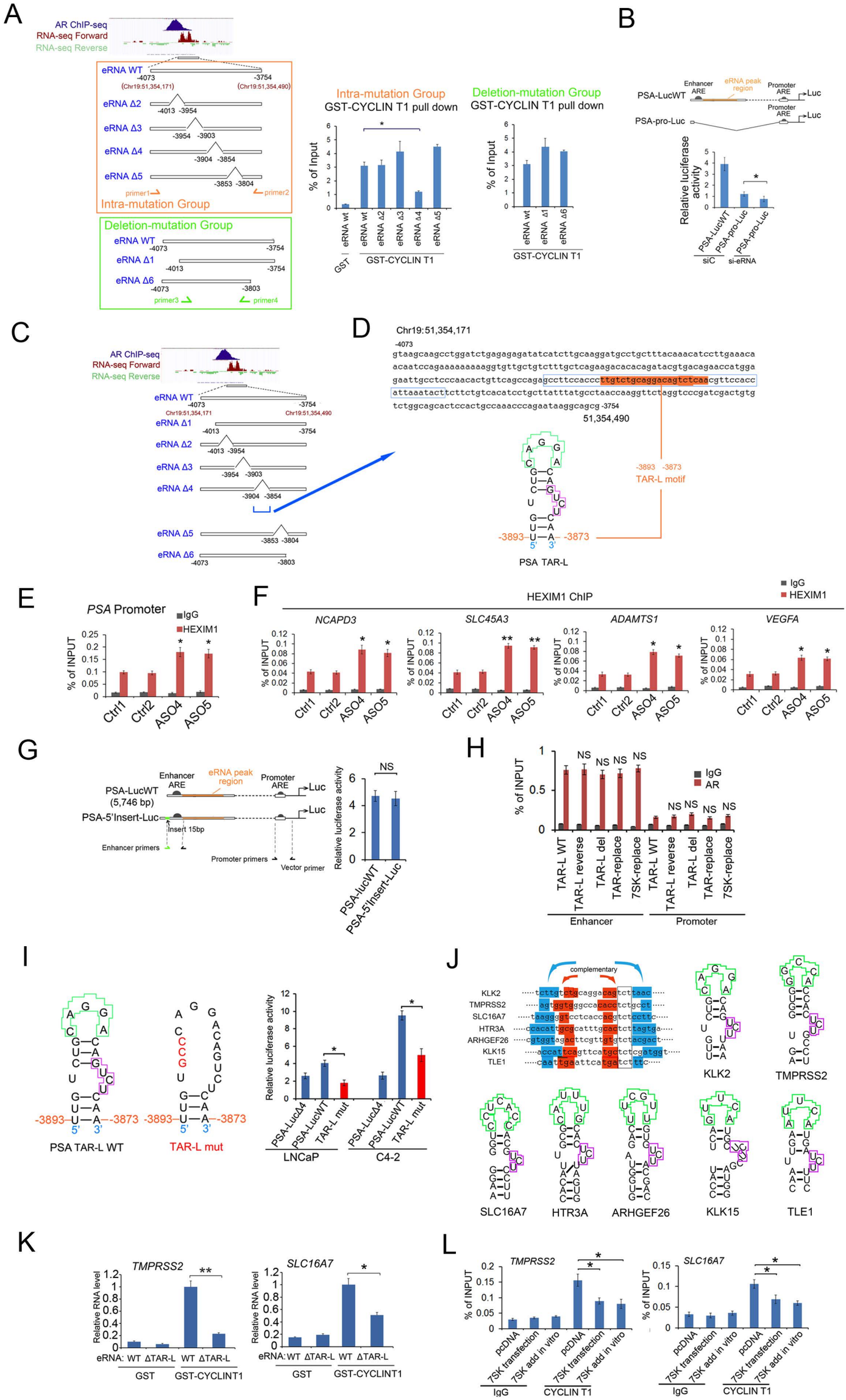

Figure S5. Binding of *PSA* eRNA to CYCLIN T1 *in vitro* and the effect of *PSA* eRNA on HEXIM1 binding at its *cis* and *trans* target loci. Related to Figure 5

(A) Left, schematic diagram of wild-type *PSA* eRNA at the peak region and the deletion mutants. The broken lines represent the deletion regions in *PSA* eRNA. Right, *in vitro* transcribed wild-type *PSA* eRNA and various deletion mutants were used for GST pulldown assays. Pulldown RNAs analyzed by RT-qPCR. All data shown are mean values ± SD (error bar) from three replicates. * $P < 0.05$.

(B) Measurement of the luciferase activity of *PSA* promoter only-luciferase reporter construct in C4-2 cells transfected with control (siC) or *PSA* eRNA-specific siRNAs. All data shown are mean values ± SD (error bar) from three replicates. * $P < 0.05$.

(C and D) Presence of a TAR-L motif in *PSA* eRNA. Location and nucleotide acid sequences (highlighted in orange) of a TAR-L motif in *PSA* eRNA. A predicted hairpin structure of the TAR-L motif in *PSA* eRNA is shown.

(E and F) HEXIM1 binding at the *PSA* and *trans* target gene promoters. C4-2 cells treated with control or *PSA* eRNA-specific ASOs were harvested for ChIP assay using IgG or HEXIM1 antibodies. Immunoprecipitated DNA was analyzed by real-time PCR. All data shown are mean values ± SD (error bar) from three replicates. * $P < 0.05$ and ** $P < 0.01$ comparing to control 1.

(G) Left, schematic diagram showing PSA-LucWT and 5'-insert mutant. Right, measurement of luciferase activity of PSA-LucWT and PSA-5'Insert-Luc in C4-2 cells. All data shown are mean values ± SD (error bar) from three replicates. NS, no significant difference.

(H) AR ChIP-qPCR analysis of AR binding at the enhancer and promoter of the *PSA* reporter genes containing a wild-type TAR-L motif or various indicated mutants. All data shown are mean values ± SD (error bar) from three replicates. NS, no significant difference.

(I) Putative structure of the wild-type and mutated TAR-L motif of *PSA* eRNA. The bases in red were mutated. Measurement of the luciferase activity of PSA-Luc reporter constructs containing an eRNA region in which the TAR-L motif was wild-type or mutated. All data shown are mean values ± SD (error bar) from three replicates. * $P < 0.05$.

(J) A predicted TAR-like motif present in eRNAs of known and new AR target genes, including *KLK2*, *TMPRSS2*, *SLC16A7*, *HTR3A*, *ARHGEF26*, *KLK15* and *TLE1*.

(K and L) Binding of CYCLIN T1 to wild-type and mutated *TMPRSS2* and *SLC16A7* eRNAs *in vitro* and *in vivo*. GST pulldown assays (K) and RIP assays in C4-2 cells (L) were performed. Pulldown RNAs were measured by RT-qPCR. All data shown are mean values ± SD (error bar) from three replicates. * $P < 0.05$.

Supplemental Fig. 6

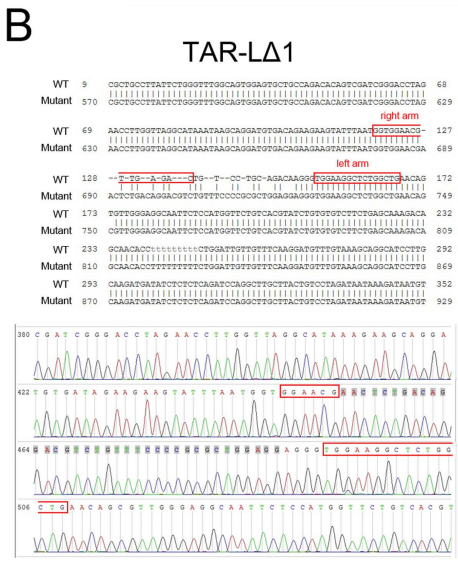

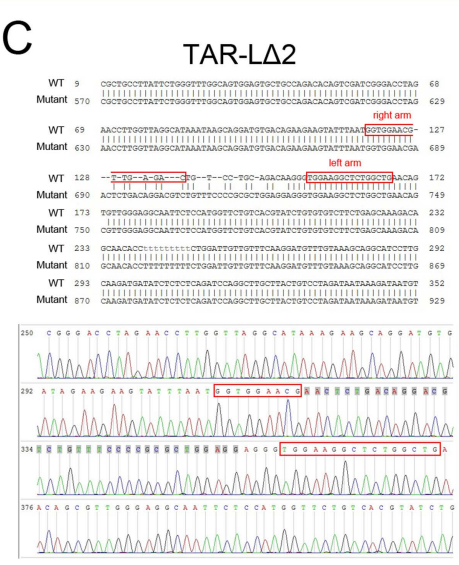

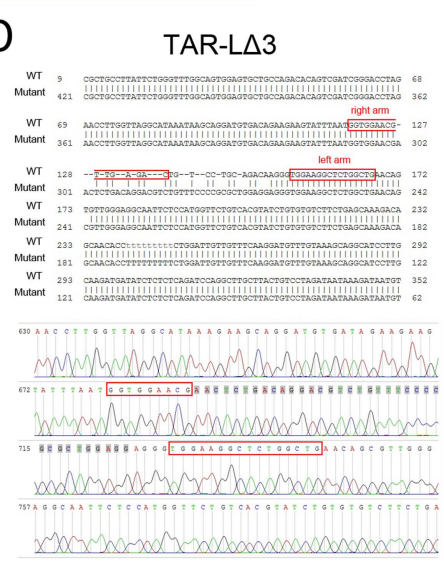

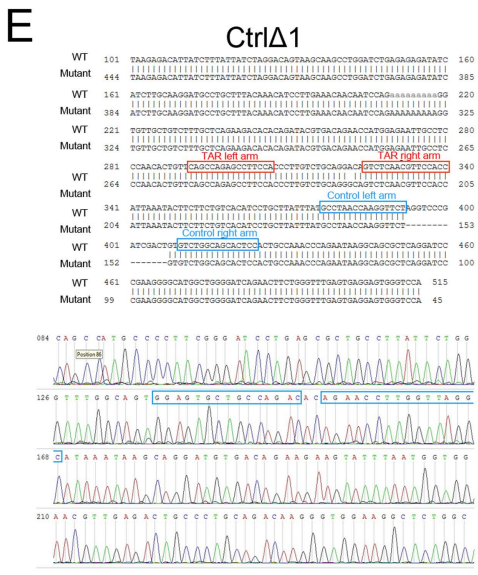

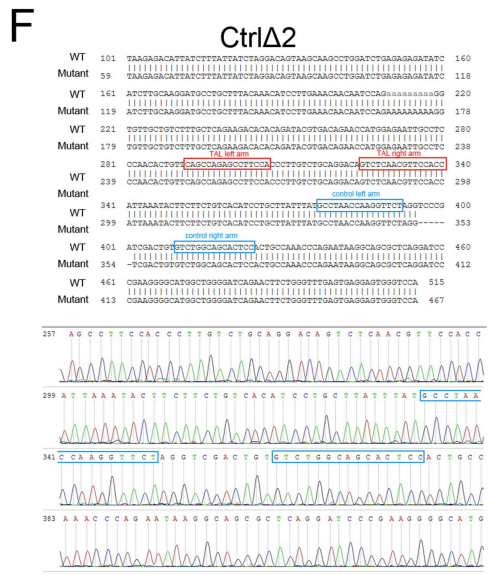

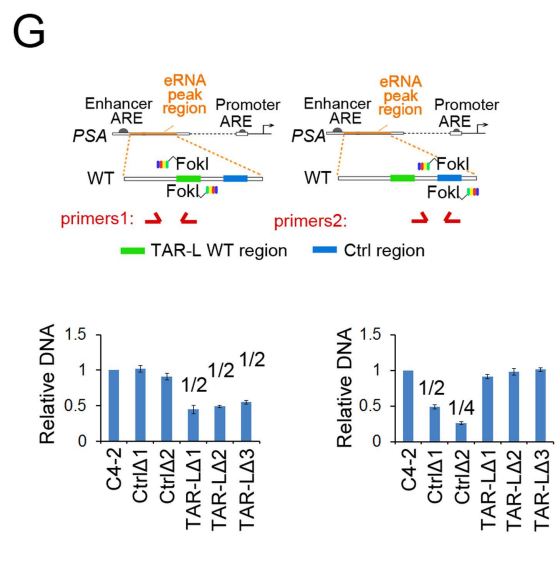

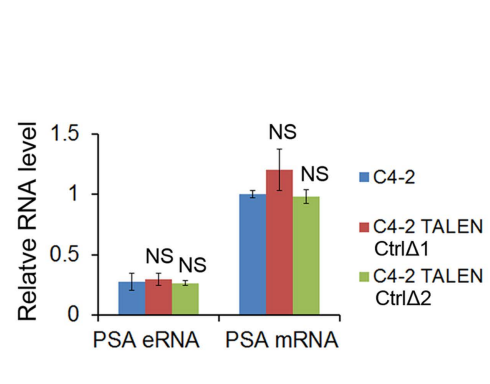

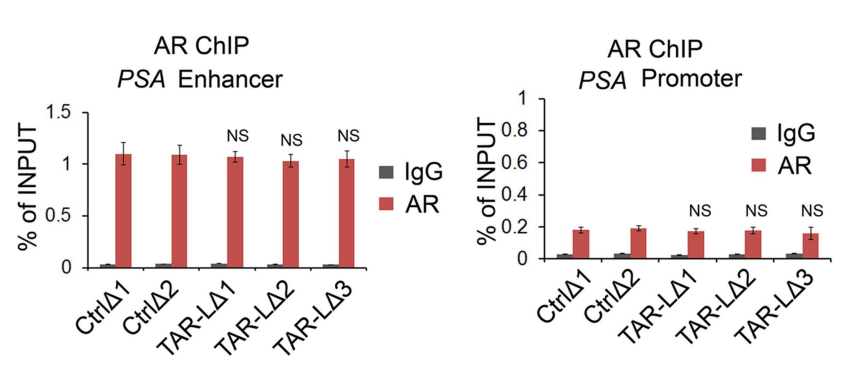

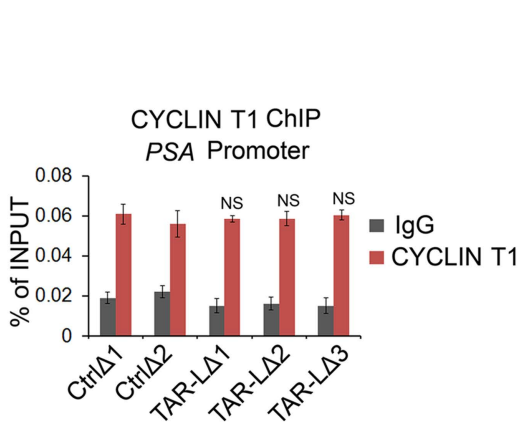

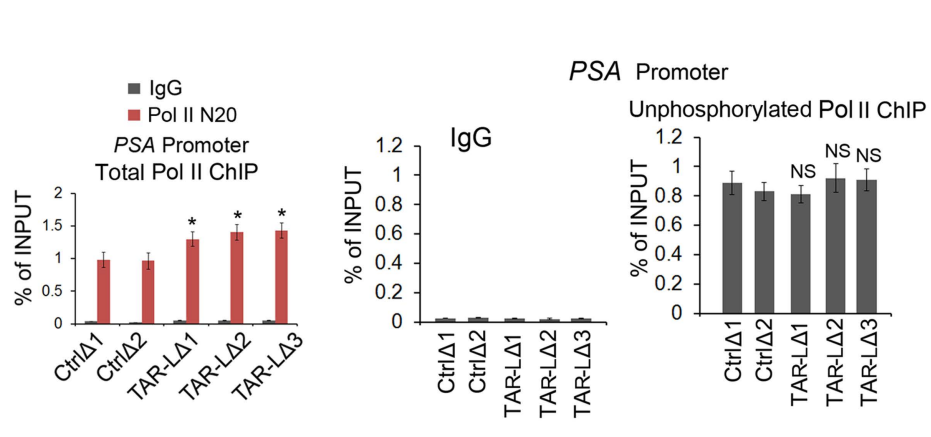

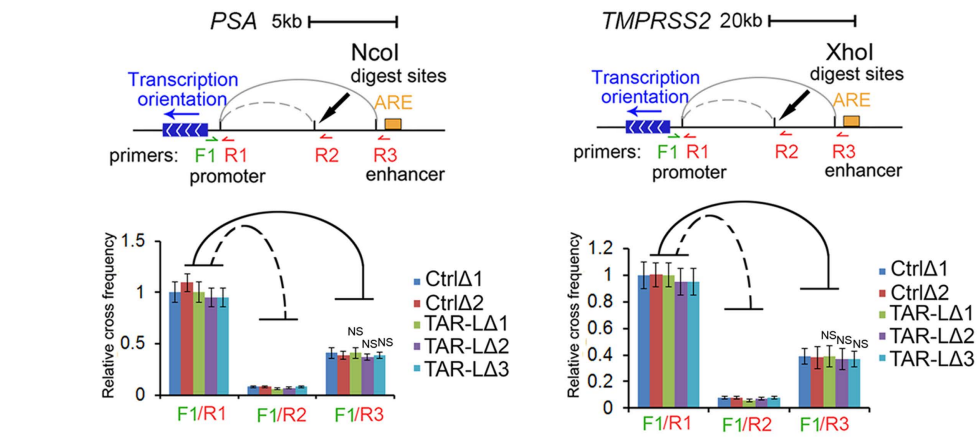

Figure S6. Generation and verification of TALEN modified C4-2 cells and the effect of TAR-L deletion at *PSA* eRNA *trans* target genes in TALEN-modified C4-2 Cells. Related to Figure 6

(A) Schematic diagram of TALEN arms to target the TAR-L motif and an adjacent downstream region in *PSA* eRNA.

(B-F) The Sanger sequencing verification of each TALEN subclone of C4-2 cells. The red boxes were TAR-L TALEN arms. The blue boxes were control TALEN arms.

(G) Real-time PCR measurement of TALEN-mediated deletion of the TAR-L motif and an adjacent control region at the genomic level in C4-2 cells.

(H) Expression of *PSA* eRNA and mRNA was measured by RT-qPCR in parental and control TALEN deletion C4-2 cell lines. All data shown are mean values ± SD (error bar) from three replicates. NS, no significant difference.

(I-K) ChIP-qPCR analysis of AR and CYCLIN T1 binding and total and unphosphorylated Pol II levels at the *PSA* gene locus in control and TAR-L deletion C4-2 cells. Immunoprecipitated DNA was detected by real-time PCR. All data shown are mean values ± SD (error bar) from three replicates. * $P < 0.05$. NS, no significant difference.

(L) Evaluation of the enhancer-promoter interaction at *PSA*, *TMPRSS2* and *NKX3.1* loci by chromosome conformation capture (3C) assays in TALEN deletion C4-2 cell lines. Solid line and dotted line show different digest sites. NS, no significant difference, comparing to control Δ1.

Supplemental Fig.7

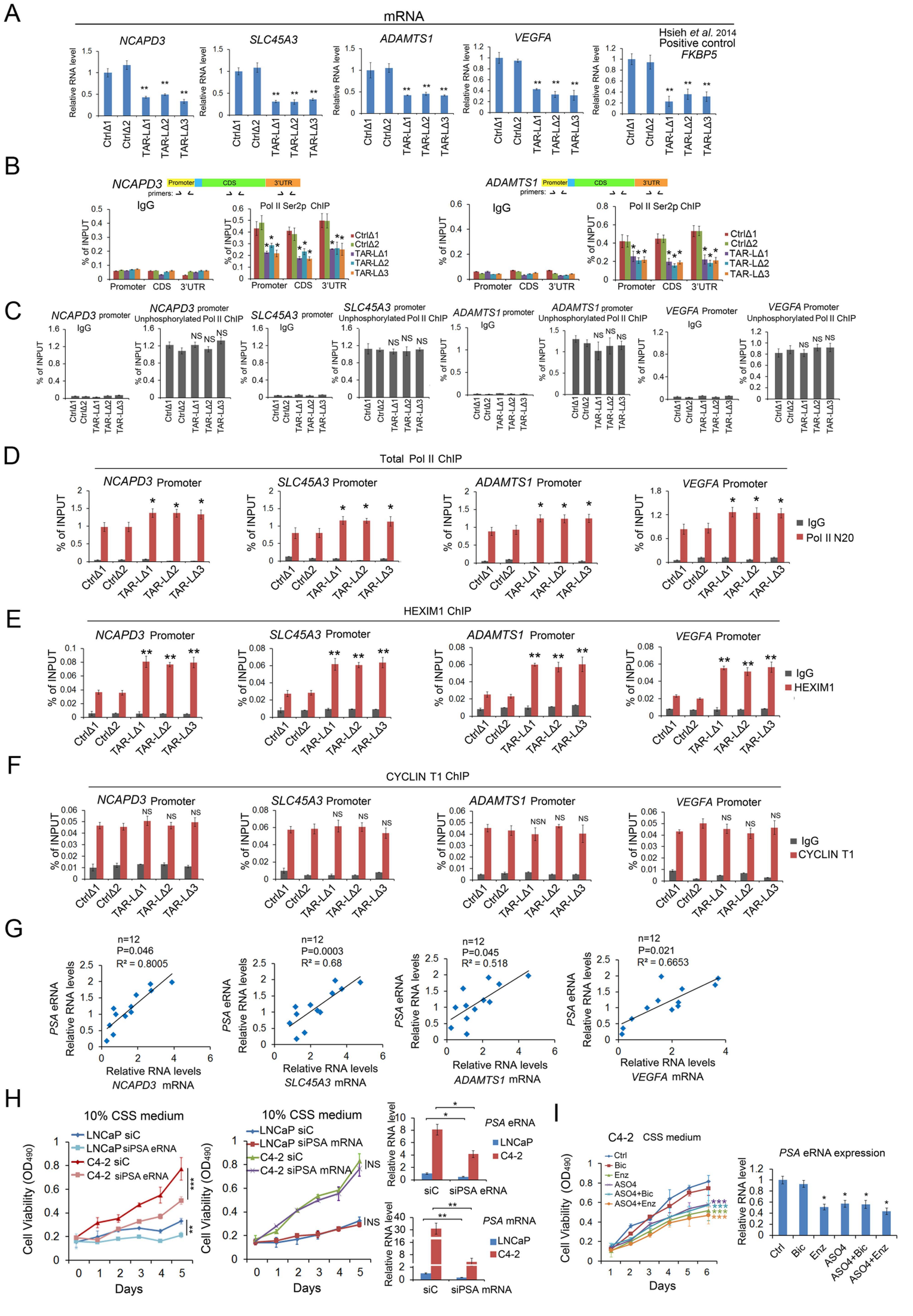

Figure S7. The effect of TAR-L deletion at *PSA* eRNA *trans* target genes in TALEN-modified C4-2 Cells. Related to Figure 6

(A) Expression of mRNAs of indicated *PSA* eRNA *trans* target genes was measured by RT-qPCR in control or TAR-L TALEN-modified C4-2 cells. All data shown are mean values ± SD (error bar) from three replicates. ** $P < 0.01$.

(B-D) ChIP-qPCR analysis of Pol II Ser2 phosphorylation, unphosphorylated Pol II (8WG16) and total Pol II (N20) at *PSA* eRNA *trans* target gene loci in C4-2 cells. TALEN-modified control or TAR-L deletion C4-2 cells were harvested for ChIP assay using anti-Pol II Ser2p, unphosphorylated Pol II (8WG16) or total Pol II (N20) antibodies. All data shown are mean values ± SD (error bar) from three replicates.* $P < 0.05$. NS, no significant difference.

(E and F) ChIP-qPCR analysis of HEXIM1 and CYCLINT1 binding at the *PSA* eRNA *trans* target gene loci in TALEN-modified cells. All data shown are mean values ± SD (error bar) from three replicates. ** $P < 0.01$. NS, no significant difference.

(G) Correlation of *PSA* eRNA expression with the mRNA expression of its *trans* target genes examined in human CRPC tissues. Total RNAs were extracted from the formalin-fixed, paraffin-embedded (FFPE). Expression of *PSA* eRNA and *trans* target gene mRNA was measured by RT-qPCR. The R^2 represents the Pearson correlation coefficient.

(H) LNCaP and C4-2 Cells were treated with control siRNAs (siC) or siRNAs for *PSA* eRNA or mRNA and the viability was measured by MTS assay. Data represent mean ± SD (error bar) from six replicates. ** $P < 0.01$; *** $P < 0.001$. The knockdown efficiencies by si-eRNA or si-mRNA were measured by RT-qPCR. Data represent mean ± SD (error bar) from three replicates. * $P < 0.05$; ** $P < 0.01$.

(I) C4-2 Cells were treated with control siRNAs (siC) or siRNAs for *PSA* eRNA in combination with bicalutamide (Bic) or enzalutamide (Enz) and the viability was measured by MTS assay. Data represent mean ± SD (error bar) from six replicates. *** $P < 0.001$ comparing with the control group. The *PSA* eRNA levels were measured by RT-qPCR. Data represent mean ± SD (error bar) from three replicates. * $P < 0.05$ comparing with the control group.

Supplementary Table 1. List of AR-eRNAs upregulated in C4-2 CRPC cells compared to androgen-dependent LNCaP cells (Fold > 2.0). Related to Figure 1.

Supplementary Table 2. List of gene loci where Pol II Ser2p levels were reduced by PSA eRNA knockdown (Genes in red are FDR < 0.001). Information regarding the loci with or without AR binding within 50-kb of the transcription start site (TSS) is also included. Related to Figure 3.

Supplementary Table 3. Gene loci (176 in total) with changes in CYCLIN T1 binding detected consistently among the replicates. Related to Figure 3.

Supplementary Table 4. Information of the primers, siRNAs/shRNAs and antibodies used in the study. Related to experimental procedures.

Supplementary Table 5. CRPC patient samples used in the study. Related to Figure 2.

Mayo Clinic		
Cases	Gleason Score	PSA
CRPC1	9	0.47
CRPC2	7	9.3
CRPC3	9	5
CRPC4	8	5.6
CRPC5	9	15.1
CRPC6	7	10.1
CRPC7	8	10
CRPC8	9	198
CRPC9	7	4.7
CRPC10	9	7.5
CRPC11	9	39.2
CRPC12	9	12.4
PCa1	10	50.2
PCa2	9	4.5
PCa3	9	13.9
PCa4	8	4.8
PCa5	8	6.6
PCa6	8	6.5
PCa7	6	6.5
PCa8	6	1.9
PCa9	6	4.2
PCa10	6	7.3
PCa11	7	5.5
PCa12	7	3.8

Changhai Samples		
Cases	Gleason Score	PSA
CRPC1	9	102
CRPC2	9	38.3
CRPC3	9	337
CRPC4	7	43
CRPC5	9	>1000
CRPC6	10	67.4
CRPC7	8	>1000
CRPC8	10	87
CRPC9	8	>1000
PCa1	7	13.5
PCa2	7	21.3
PCa3	7	9.2
PCa4	7	7.5
PCa5	7	8.4
PCa6	7	11.8

PCa7	7	5.3
PCa8	7	15.2

SUPPLEMENTAL EXPERIMENTAL PROCEDURES

Plasmids, reagents and antibodies

GST-tagged Pol II C-terminal domain, CDK9 and CYCLIN T1 were generated by cloning the corresponding cDNAs into pGEX-4T-1 vector. The cDNA fragments were amplified by Phusion polymerase (NEB, USA) using Phusion High-Fidelity PCR Master Mix. Mammalian expression plasmids for *PSA*, *TMPRSS2* and *SLC16A7* eRNA, *PSA* mRNA, Flag-CDK9 and *7SK* snRNA were generated by inserting each target cDNA into the pcDNA3.1 vector. The PSA-5746-luciferase plasmid (PSA-LucWT) was reported previously (Liu et al., 2008). The insert and deletion mutants of PSA-Luc were constructed using KOD-plus-Mutagenesis Kit (TOYOBO, Japan). The primers used for plasmid construction and mutagenesis are shown in the Table S4. AR (Santa Cruz sc-816), ARHGEF26 (Sigma HPA017722), CDK7 (Santa Cruz sc-529), CDK9 (Santa Cruz sc-484), CDK9 T186 (Abcam ab79178), CDK12 (Cell signaling #11973), CYCLINT1 (Santa Cruz sc-10750), ERK2 (Santa Cruz sc-1647), FCP1 (Santa Cruz sc-32867), HEXIM1 (Abcam ab25388), HTR3A (Abcam ab45314), KLK15 (Abcam ab28570), NELF-E (Abcam ab170104), Pol II 8WG16 (Covance MMS-126R), Pol II N20 (Santa Cruz sc-899), Pol II ser2p (Abcam ab5095), Pol II ser2p for ChIP-seq (Covance MMS-129R),Pol II ser5p (Abcam ab5131), SLC16A7 (Sigma SAB2500948), Streptavidin-HRP (Cell Signaling #3999), and TLE1(Santa Cruz sc-13368).

Cell lines, cell culture and reagents

Cells were cultured in RPMI 1640 medium supplemented with 10% charcoal-stripped fetal bovine serum (FBS) (Invitrogen) (androgen-depleted medium) and 100 µg/ml penicillin-streptomycin-glutamine (Invitrogen) at 37ºC with 5% CO2.

Human prostate cancer specimens and RNA isolation from human tissues

Formalin-fixed paraffin-embedded (FFPE) hormone-naïve primary prostate cancer and CRPC tissues were randomly selected from the Mayo Tissue Registry. Hormone-naïve patients with biopsy-proven prostate cancer have been treated at Mayo Clinic by radical retropubic prostatectomy between January 1995 and December 1998 without neoadjuvant therapy. The study was approved by the Mayo Clinic Institutional Review Board. Clinical tissue specimens from Chinese patients were obtained from the frozen archives of Shanghai Changhai Hospital with the approval of the Medical Ethics Committee and with informed consent. Detailed patient information can be seen in Table S5. FFPE tissues were collected and total RNAs were isolated using a RecoverAll Total Nucleic Acid Isolation Kit (Life Technologies). Isolation of RNAs from frozen human prostate cancer tissues was performed as described previously (Jiao et al., 2014).

Prostate cancer xenografts LuCaP23.1 and 23.1AI

Patient-derived androgen dependent (AD) LuCaP23.1 and castration-resistant (or androgen independent, AI) LuCaP23.1 AI xenograft models were kindly provided by Dr. Robert L. Vessella (Department of Urology, University of Washington Medical Center, Seattle, WA). AD LuCaP xenografts were propagated in BALB/c nu/nu mice and AI xenografts were propagated in SCID mice. Mice were housed in the Mayo Clinic pathogen-free rodent facility. All procedures were approved by the Mayo Clinic Institutional Animal Care and Use Committee (IACUC).

Design and screening of highly optimized generation-2.5 antisense oligonucleotides (ASOs)

All ASOs used in this study contained a full phosphorothioate backbone and a 10-base 2′-deoxynucleoside gap flanked by 2′-*O*-ethyl (cEt)-modified nucleotides. The motif for the ASOs targeting the *PSA* (or *KLK3)* eRNA tested was mmm-10-mmm, where m represents cEt modification and -10- represents the 10-base DNA gap. ASOs were synthesized and purified as described previously (Baker et al., 1997; Seth et al., 2008). A large number of ASOs targeting sense-strand *PSA* eRNA were screened by Ionis Pharmaceuticals Inc. (Carlsbad, CA) for high efficient reduction of *PSA* eRNA. ASO4 (5′-ATGGTGCTGGCCACAC-3’) and ASO5 (5′-GAACCTTGGTTAGGCA-3’) that resulted in strong reduction of *PSA* eRNA were selected for further studies. Two negative control ASOs (5’-GACGCGCCTGAAGGTT-3’ and 5’-GGCTACTACGCCGTCA-3’) with the same chemistry, but matching no human transcripts, Control-1 and -2 were included in each experiment to demonstrate the specificity of *PSA* eRNA ASOs. All oligonucleotides were designed to exclude G-strings with four Gs or two sets of three Gs in a row to prevent non-antisense-mediated effects (Baker et al., 1997).

Transcription activator-like effector nuclease (TALEN) construction

TALENs were designed using Mojo Hand software using the following settings (minimum spacer length 14 bp, maximum spacer length 19 bp, minimum binding length 15 bp, maximum binding length 16 bp) (Neff et al., 2013). TALENs were designed to target unique restriction sites within the TAR-L motif of *PSA* eRNA and its 3’ adjacent

region. Cutting efficiency was assayed using restriction fragment length polymorphism (RFLP) analysis. One TALEN pair was designed to target a critical hairpin in the TAR-L motif and the other 70 bp downstream of this region, which was designed to serve as an internal control. TALENs were assembled using a modified Golden Gate Assembly system that used libraries of every possible combination of 3-mer TALE RVD monomers (RVDs: NI, HD, NN and NG) packaged in a 4 vector system (pFUSX1-4) along with a dimer (pFusX_B2) or trimer library (pFusX_B3), and the terminal RVD half repeat. Using this modified system, a derivative of the Golden Gate TALEN and TAL Effector Kit 2.0, any possible 15 and 16-RVD TALEN can be constructed rapidly in a single reaction within three days and is backward compatible with the current Golden Gate Assembly kit (Cermak et al., 2011; Ma et al., 2013). TALENs were assembled in the highly efficient pC-GoldyTALEN backbone (Bedell et al., 2012).

Generation of TALEN modified C4-2 cells

C4-2 cells were transfected with TALEN vectors and selected with puromycin. Pooled cells will be pre-screened for the effectiveness of TALEN-mediated DNA editing by purifying genomic DNA for RFLP analysis using PstI and PvuI. Screening-positive cells were subject to series dilution for the purpose of isolation of single cell clones. Genomic DNA was isolated from each individual cell clone and RFLP was performed. For RFLP screen-positive clones, PCR products were amplified from the deletion targeting regions and subcloned into the pGEM-T Easy vector (Promega) for Sanger sequencing to confirm the deletion of the target region.

***In vitro* transcription and RNA pulldown by GST recombinant proteins**

A genomic fragment, corresponding to the *PSA* eRNA signal peak region in the *PSA* gene locus (from 51,354,171 to 51,354,490 on chromosome 19), was subcloned into the pcDNA3.1 backbone vector. Mutations with various deletions within this region were generated by mutagenesis using a KOD-Plus-Mutagenesis Kit (TOYOBO). Wild-type and mutated vectors were linearized by digestion with XbaI and purified by the Gel Extraction Kit (Qiagen). 200 ng linearized plasmid DNAs were transcribed *in vitro* using T7 RNA polymerase. RNAs were treated with DNase I to eliminate the template DNA. GST-CYCLIN T1 and GST-CDK9 recombinant proteins were expressed in *E. coli* (BL21) after induction with 0.5 mM IPTG at 16ºC for 12 h and purified with glutathione Sepharose 4B beads (GE Healthcare) as described previously (Wang et al., 2013). Purified GST recombinant proteins were incubated with *in vitro* transcribed RNA in RNA structure buffer (50 mM Tris, pH 7.4; 150 mM NaCl; 1 mM $MgCl_2$) (Wan et al., 2014). For the GST-CYCLIN T1 binding assay, $ZnCl_2$ was added to the binding buffer to a final concentration of 1 mM. After extensive washes, RNAs were purified using the RNeasy MinElute Cleanup Kit (Qiagen). Precipitated RNA was detected by real-time RT-PCR.

RNA isolation from cultured cells, reverse transcription PCR (RT-PCR) and real-time PCR

Total RNA was isolated from cultured cells using TRIzol reagent (Invitrogen) or the RNeasy Plus Mini Kit (Qiagen) according to the manufacturer's instructions. First-strand cDNA was synthesized with the PrimeScript Reverse Transcriptase Kit (TaKaRa Bio). Reverse transcription and real-time PCR were performed as described previously (Wang et al., 2013). The PCR primers for AR new target genes are listed in Table S4.

Biotin-labeled RNA pulldown and western blot analysis

RNAs were biotin-labeled during *in vitro* transcription using Biotin RNA Labeling Mix (Roche) and T7 polymerase (New England Biolabs). C4-2 cells cultured in androgen-depleted medium were lysed in modified Binding buffer (50mM Tris-HCl pH7.5, 150mM NaCl, 1% NP-40, 0.1% SDS and 1% protease inhibitor cocktails). Cell lysates were incubated with biotin-labelled RNAs and streptavidin beads at 4ºC for 12 h. The beads were washed in wash buffer (50 mM Tris, pH 7.4; 150 mM NaCl; 0.05% Nonidet P-40 (NP-40); 1mM $MgCl_2$) at 4ºC six times. The samples were subjected to western blot analyses as described previously (Wang et al., 2013). Briefly, protein samples were denatured and subjected to SDS-polyacrylamide gel electrophoresis (SDS/PAGE), and were transferred to nitrocellulose membranes (Bio-Rad). The membranes were immunoblotted with specific primary antibodies, horseradish peroxidase-conjugated secondary antibodies, and visualized by SuperSignal West Pico Stable Peroxide Solution (Thermo Scientific). The antibodies are shown in Table S4.

SFB-CDK9 and GST-Pol II-C preparation

293T cells were transfected with plasmids encoding SFB-tagged CDK9 (S-tag, Flag epitope tag, and streptavidin-binding peptide tag) to establish cell lines expressing tagged proteins. Cells were lysed in NETN buffer (20 mM Tris-HCl at pH 8.0, 100 mM NaCl, 0.5% Nonidet P-40, 1 mM EDTA) containing 50 mM β-glycerophosphate, 10 mM NaF, and 1 μg/mL each of pepstatin A and aprotinin. Following centrifugation, the pellet was sonicated for 1

min in high-salt solution (20 mM HEPES at pH 7.8, 0.4 M NaCl, 1 mM EGTA, 1 mM EDTA, protease inhibitor) to extract proteins. The supernatants were cleared at 13,000 rpm to remove debris and then incubated with streptavidin-conjugated beads (GE Healthcare Life Sciences) for 1 h at 4°C. The immunocomplexes were washed three times with NETN buffer and then bead-bound proteins were eluted with NETN buffer containing 2 mg/mL biotin (Sigma). After elution, the immunocomplexes were analyzed by SDS-PAGE and prepared for Pol II CTD kinase assay. 372 amino acids of Pol II C-terminal domain (Pol II-C) were cloned into the pFEX-4T1 plasmid to make a GST-Pol II-C recombinant protein. GST-Pol II-C recombinant proteins were expressed in *E. coli* (BL21) after induction with 0.5 mM IPTG at 16ºC for 12 h and purified with glutathione Sepharose 4B beads (GE Healthcare) as described previously (Wang et al., 2013). Purified GST recombinant proteins were prepared for Pol II CTD kinase assay.

Pol II CTD kinase assay

GST or GST-Pol II-C terminal domain (GST-Pol II-C, 372 amino acids of the Pol II-C terminal domain) recombinant proteins were incubated with CDK9 immunoprecipitated from cells for kinase assay using the method as described previously (Murray et al., 2001). The kinase reaction mixtures added with or without 1 µg *in vitro* transcribed *PSA* eRNA were incubated at 30°C for 30 min and then stopped by the addition of SDS-PAGE buffer. The samples were measured using western blotting.

Chromatin immunoprecipitation (ChIP) and chromatin isolation by RNA purification (ChIRP)

ChIP was performed as described previously (Boyer et al., 2005). The ChIRP experiment was performed essentially as per the original protocol as described previously (Chu et al., 2011). The online Biosearch Technologies' Stellaris FISH Probe Designer was used to design antisense oligo probes tiling *PSA* eRNA. The probe oligos were synthesized with a 3'-Biotin-TEG modification and purified by HPLC. The ChIP primers and ChIRP probes are shown in Table S4.

RNA-seq and data analysis

LNCaP and C4-2 cells were cultured in androgen-depleted media for 72 h. Total RNAs were isolated from cells using the methods as described previously (Wang et al., 2013). Briefly, RNA was isolated using RNeasy Plus Mini Kit (Qiagen). High quality (Agilent Bioanalyzer RIN >7.0) total RNAs were employed for the preparation of sequencing libraries using Illumina TruSeq Stranded Total RNA/Ribo-Zero Sample Prep Kit. A total of 500–1,000 ng of riboRNA-depleted total RNA was fragmented by RNase III treatment at 37^{o}C for 10–18 min and RNase III was inactivated at 65^{o}C for 10 min. Size selection (50 to 150 bp fragments) was performed using the FlashPAGE denaturing PAGE-fractionator (Life Technologies) prior to ethanol precipitation overnight. The resulting RNA was directionally ligated, reverse-transcribed and RNase H treated.

Samples with biological duplicates were sequenced using the Illumina HiSeq2000 platform at the Mayo Genome Core Facility. Pre-analysis quality control was performed using FastQC (http://www.bioinformatics.babraham.ac.uk/projects/fastqc/) and RSeQC software (Wang et al., 2012) to ensure that raw data are in excellent condition and suitable for downstream analyses. Pair-end raw reads were aligned to the human reference genome (GRch37/hg19) using Tophat (Trapnell et al., 2009). Genome-wide coverage signals were represented in BigWig format to facilitate convenient visualization using the UCSC genome browser. Gene expression was measured using RPKM (Reads Per Kilo-base exon per Million mapped reads) as described previously (Mortazavi et al., 2008). Correlation analyses between eRNA and mRNA expression were performed using Python and R scripts. EdgeR (Robinson and Oshlack, 2010) was used to identify genes that were differentially expressed between CRPC and primary prostate tumors. Raw and processed data have been deposited into NCBI Gene Expression Omnibus with accession number GSE55032.

ChIP-seq and data analysis, and ChIP-qPCR

ChIP-seq libraries were prepared using the methods as described previously (Boyer et al., 2005) and high throughput sequencing was performed using the Illumina HiSeq2000 platforms at the Mayo Genome Core Facility. The data were analyzed using the following pipeline: (1) Mapping. ChIP-seq raw reads were aligned to reference genome (GRCh37/hg19) using Burrows-Wheeler Alignment (BWA) tool (Li and Durbin, 2009). (2) Quality control. Subsequent to alignments, the following factors were evaluated to ensure that the sequencing data were of sufficient quality for downstream applications: the number of reads that can be mapped to unique locations in the genome, the number of nonredundant reads and the saturation test of sequencing depth. The saturation test was used to decide if current sequencing depth is sufficient to capture all protein binding locations. (3) Peak detection and visualization. MACS (Zhang et al., 2008) was used to perform peak calling because it has been demonstrated to work very well

with sharp peaks for transcription regulatory proteins (such as AR). BigBed and BigWig files were generated to facilitate both easy processing and high performance visualization with the UCSC genome browser or IGV. Integration of AR ChIP-seq data with other published epigenetic datasets such as histone ChIP-seq, FOXA1 ChIP-seq was performed using Epidaurus (Wang et al., 2014). For ChIP-qPCR experiments, DNAs pulled down by antibodies were amplified by real-time PCR. PCR primers at the enhancer and promoters of AR-related genes are shown in Table S4. Raw and processed data have been deposited into NCBI Gene Expression Omnibus with accession number GSE55032.

Luciferase reporter gene assays

For luciferase reporter gene assays, cells (2×10^5 cells per well in 6-well plates) were transfected with *PSA* wild type (WT) and mutated firefly luciferase reporter plasmids (1 μg) and the pRL-TK renilla luciferase reporter normalization construct (0.01 μg) using Lipofectamine 2000 (Invitrogen). For *PSA* eRNA knockdown experiments, non-specific and *PSA* eRNA-specific siRNAs (50 nM/each) were co-transfected with reporter plasmids. At 48 h after transfection, luciferase activities were measured using a Dual-Luciferase Reporter Assay Kit (Promega). Data were presented as firefly luciferase activity normalized to Renilla luciferase activity for each set of triplicate samples. All experiments were performed at least five times.

RNA immunoprecipitation (RIP) assay

RIP was performed as described previously (Wang et al., 2013). Briefly, cell were lysed with RIP buffer (150 mM NaCl, 25 mM Tris pH 7.4, 5 mM EDTA, 0.5 mM DTT, 0.5% NP-40, 100 U/ml RNase inhibitor) on ice for 35 min. For sonication RIP, cells were crosslinked with 0.1% formaldehyde for 10 min prior to lysis. The cell lysates were sonicated to solubilize and shear crosslinked RNA for 15 min. The protein-RNA mixture was incubated with antibodies and protein G beads overnight. The beads were washed with RIP buffer six times. The RNAs were extracted with RNeasy MinElute Cleanup Kit (Qiagen). First-strand cDNA was synthesized using the PrimeScript Reverse Transcriptase Kit (TaKaRa Bio). Reverse transcription and real-time PCR were performed as described previously (Wang et al., 2013) . The PCR primers for *PSA* eRNAs are listed in Table S4.

Quantitative chromosome conformation capture (3C) Assay

3C assays were performed as described previously (Hagege et al., 2007). Briefly, the crosslinked chromatin was digested with specific restriction enzymes overnight. The crosslinking was reversed and ligated DNA was purified. Primers for qPCR are listed in Table S4.

RNA dot blot hybridization

The dot blot assays were performed as described previously (Liu et al., 2013). Briefly, equal amounts of biotin-labelled RNA were dot blotted and the blot was incubated with the Streptavidin-HRP antibody for 2 h and visualized by SuperSignal West Pico Stable Peroxide Solution (Thermo Scientific). Antibodies for dot blot are listed in Table S4.

MTS assay

The MTS assays were performed according to manufacturer's instructions (Promega). Briefly, cells were plated in 96-well plates at a density of 2,000 cells per well. At the indicated times, 20 μl of CellTiter 96R AQ_{ueous} Solution Reagent (Promega) was added to each well, and incubated for 2 h at 37 C in the cell incubator and then was measured in a microplate reader at 490 nm.

eRNA copy number measurement and nuclear extract isolation

The *PSA* eRNA peak region (350 bp) and *PSA* mRNA was cloned into the pcDNA3.1 backbone vector, using the primers provided in Table S4. The cDNA copy number and dilution calculation was performed using the method described in https://www.lifetechnologies.com/us/en/home/brands/thermo-scientific/molecular-biology/molecular-biology-learning-center/molecular-biology-resource-library/thermo-scientific-web-tools/dna-copy-number-calculator.html. 1×10^5 cells were used for RNA extraction from whole cells or isolated nuclei using RNeasy Plus Mini Kit (Qiagen). Isolation of Nuclei were performed by treating cells with the extraction buffer (10 mM HEPES (pH 7.9), 1.5 mM $MgCl_2$, 10 mM KCl, 0.5 mM DTT, 0.05% NP-40, 100 U/ml RNase inhibitor and 1% protease inhibitor cocktails) on ice for 10 min, followed by centrifuge at 300 rpm for 10 min. RNAs were diluted in 100 μl DEPC H_2O and 1 μl of 100 μl was used for reverse transcription. cDNA was diluted into 100 μl, and 1 μl was used for qPCR. Thus the final Ct value means the DNA copy number in 10 cells. Considering that the efficiency of reverse transcriptase (RT) on mRNA of genes such as *GAPDH* is estimated to be approximately 50% (Zhong et al.,

2008), which might be even lower for expression levels of eRNAs examined, the real copy numbers of *PSA* eRNA could be higher than the estimation.

Statistical analysis

Experiments were carried out with three or more replicates unless otherwise stated. Statistical analyses were performed using Student's *t* test for most comparisons. $P < 0.05$ is considered statistically significant. Non-parametric Kolmogorov-Smirnov (KS) test was used to evaluate statistical significance of differential expression between primary prostate cancer and CRPC.

Supplemental References

Baker, B.F., Lot, S.S., Condon, T.P., Cheng-Flournoy, S., Lesnik, E.A., Sasmor, H.M., and Bennett, C.F. (1997). 2'-O-(2-Methoxy)ethyl-modified anti-intercellular adhesion molecule 1 (ICAM-1) oligonucleotides selectively increase the ICAM-1 mRNA level and inhibit formation of the ICAM-1 translation initiation complex in human umbilical vein endothelial cells. J. Biol. Chem. *272*, 11994-12000.

Bedell, V.M., Wang, Y., Campbell, J.M., Poshusta, T.L., Starker, C.G., Krug, R.G., 2nd, Tan, W., Penheiter, S.G., Ma, A.C., Leung, A.Y., *et al.* (2012). In vivo genome editing using a high-efficiency TALEN system. Nature *491*, 114-118.

Boyer, L.A., Lee, T.I., Cole, M.F., Johnstone, S.E., Levine, S.S., Zucker, J.P., Guenther, M.G., Kumar, R.M., Murray, H.L., Jenner, R.G., *et al.* (2005). Core transcriptional regulatory circuitry in human embryonic stem cells. Cell *122*, 947-956.

Cermak, T., Doyle, E.L., Christian, M., Wang, L., Zhang, Y., Schmidt, C., Baller, J.A., Somia, N.V., Bogdanove, A.J., and Voytas, D.F. (2011). Efficient design and assembly of custom TALEN and other TAL effector-based constructs for DNA targeting. Nucleic Acids Res. *39*, e82.

Chu, C., Qu, K., Zhong, F.L., Artandi, S.E., and Chang, H.Y. (2011). Genomic maps of long noncoding RNA occupancy reveal principles of RNA-chromatin interactions. Mol. Cell *44*, 667-678.

Glinsky, G.V., Berezovska, O., and Glinskii, A.B. (2005). Microarray analysis identifies a death-from-cancer signature predicting therapy failure in patients with multiple types of cancer. J. Clin. Invest. *115*, 1503-1521.

Grasso, C.S., Wu, Y.M., Robinson, D.R., Cao, X., Dhanasekaran, S.M., Khan, A.P., Quist, M.J., Jing, X., Lonigro, R.J., Brenner, J.C., *et al.* (2012). The mutational landscape of lethal castration-resistant prostate cancer. Nature *487*, 239-243.

Hagege, H., Klous, P., Braem, C., Splinter, E., Dekker, J., Cathala, G., de Laat, W., and Forne, T. (2007). Quantitative analysis of chromosome conformation capture assays (3C-qPCR). Nat. Protoc. *2*, 1722-1733.

Hsieh, C.L., Fei, T., Chen, Y., Li, T., Gao, Y., Wang, X., Sun, T., Sweeney, C.J., Lee, G.S., Chen, S., *et al.* (2014). Enhancer RNAs participate in androgen receptor-driven looping that selectively enhances gene activation. Proc. Natl. Acad. Sci. U S A *111*, 7319-7324.

Jiao, L., Deng, Z., Xu, C., Yu, Y., Li, Y., Yang, C., Chen, J., Liu, Z., Huang, G., Li, L.C., *et al.* (2014). miR-663 induces castration-resistant prostate cancer transformation and predicts clinical recurrence. J. Cell Physiol. *229*, 834-844.

Li, H., and Durbin, R. (2009). Fast and accurate short read alignment with Burrows-Wheeler transform. Bioinformatics *25*, 1754-1760.

Liu, P., Li, S., Gan, L., Kao, T.P., and Huang, H. (2008). A transcription-independent function of FOXO1 in inhibition of androgen-independent activation of the androgen receptor in prostate cancer cells. Cancer Res. *68*, 10290-10299.

Liu, W., Ma, Q., Wong, K., Li, W., Ohgi, K., Zhang, J., Aggarwal, A.K., and Rosenfeld, M.G. (2013). Brd4 and JMJD6-associated anti-pause enhancers in regulation of transcriptional pause release. Cell *155*, 1581-1595.

Ma, A.C., Lee, H.B., Clark, K.J., and Ekker, S.C. (2013). High efficiency In Vivo genome engineering with a simplified 15-RVD GoldyTALEN design. PLoS One *8*, e65259.

Mortazavi, A., Williams, B.A., McCue, K., Schaeffer, L., and Wold, B. (2008). Mapping and quantifying mammalian transcriptomes by RNA-Seq. Nature Methods *5*, 621-628.

Murray, S., Udupa, R., Yao, S., Hartzog, G., and Prelich, G. (2001). Phosphorylation of the RNA polymerase II carboxy-terminal domain by the Bur1 cyclin-dependent kinase. Mol. Cell Biol. *21*, 4089-4096.

Neff, K.L., Argue, D.P., Ma, A.C., Lee, H.B., Clark, K.J., and Ekker, S.C. (2013). Mojo Hand, a TALEN design tool for genome editing applications. BMC Bioinformatics *14*, 1.

Robinson, M.D., and Oshlack, A. (2010). A scaling normalization method for differential expression analysis of RNA-seq data. Genome Biol. *11*, R25.

Seth, P.P., Siwkowski, A., Allerson, C.R., Vasquez, G., Lee, S., Prakash, T.P., Kinberger, G., Migawa, M.T., Gaus, H., Bhat, B., *et al.* (2008). Design, synthesis and evaluation of constrained methoxyethyl (cMOE) and constrained ethyl (cEt) nucleoside analogs. Nucleic Acids Symp. Ser. (Oxf), 553-554.
Trapnell, C., Pachter, L., and Salzberg, S.L. (2009). TopHat: discovering splice junctions with RNA-Seq. Bioinformatics *25*, 1105-1111.
Wan, Y., Qu, K., Zhang, Q.C., Flynn, R.A., Manor, O., Ouyang, Z., Zhang, J., Spitale, R.C., Snyder, M.P., Segal, E., *et al.* (2014). Landscape and variation of RNA secondary structure across the human transcriptome. Nature *505*, 706-709.
Wang, D., Garcia-Bassets, I., Benner, C., Li, W., Su, X., Zhou, Y., Qiu, J., Liu, W., Kaikkonen, M.U., Ohgi, K.A., *et al.* (2011). Reprogramming transcription by distinct classes of enhancers functionally defined by eRNA. Nature *474*, 390-394.
Wang, L., Huang, H., Dougherty, G., Zhao, Y., Hossain, A., and Kocher, J.P. (2014). Epidaurus: aggregation and integration analysis of prostate cancer epigenome. Nucleic Acids Res. *43*, e7.
Wang, L., Wang, S., and Li, W. (2012). RSeQC: quality control of RNA-seq experiments. Bioinformatics *28*, 2184-2185.
Wang, L., Zeng, X., Chen, S., Ding, L., Zhong, J., Zhao, J.C., Sarver, A., Koller, A., Zhi, J., Ma, Y., *et al.* (2013). BRCA1 is a negative modulator of the PRC2 complex. The EMBO J. *32*, 1584-1597.
Yu, Y.P., Landsittel, D., Jing, L., Nelson, J., Ren, B., Liu, L., McDonald, C., Thomas, R., Dhir, R., Finkelstein, S., *et al.* (2004). Gene expression alterations in prostate cancer predicting tumor aggression and preceding development of malignancy. J. Clin. Oncol. *22*, 2790-2799.
Zhang, Y., Liu, T., Meyer, C.A., Eeckhoute, J., Johnson, D.S., Bernstein, B.E., Nusbaum, C., Myers, R.M., Brown, M., Li, W., *et al.* (2008). Model-based analysis of ChIP-Seq (MACS). Genome Biol. *9*, R137.
Zhong, J.F., Chen, Y., Marcus, J.S., Scherer, A., Quake, S.R., Taylor, C.R., and Weiner, L.P. (2008). A microfluidic processor for gene expression profiling of single human embryonic stem cells. Lab. Chip *8*, 68-74.